# Interband Faraday effect in $Cd_{1-x}Mn_xSe$

Eunsoon Oh, D. U. Bartholomew, and A. K. Ramdas
*Department of Physics, Purdue University, West Lafayette, Indiana 47907*

J. K. Furdyna and U. Debska
*Department of Physics, University of Notre Dame, Notre Dame, Indiana 46556*

(Received 1 August 1988)

The interband Faraday rotation in the uniaxial diluted magnetic semiconductor $Cd_{1-x}Mn_xSe$, measured with the direction of propagation $\hat{\mathbf{k}}$ and the magnetic field $\mathbf{H}$ along its optic axis ($\hat{\mathbf{c}}$), has been investigated for $0 \le x < 0.5$. The Faraday rotation, positive for CdSe, becomes negative and very large when $Mn^{2+}$ replaces $Cd^{2+}$. The sign of the rotation and its dependence on $x$, $H$, and temperature $T$ are dominated by the spin-spin exchange interaction between the spins of the $3d$ electrons of $Mn^{2+}$ and those of the band electrons. The dispersion of the Verdet constant is well described by the excitonic model (single-oscillator model). The antiferromagnetic coupling between $Mn^{2+}$ ions is manifested in the Faraday effect through the phenomenological effective temperature $(T+T_{AF})$, as well as with hysteresis effects associated with the formation of a spin-glass phase for high $x$ and low $T$.

## I. INTRODUCTION

Diluted magnetic semiconductors (DMS's) are alloys of nonmagnetic and magnetic compounds. In recent years, there has been much interest in DMS alloys in which the group-II element of a II-VI crystal is in part replaced by a transition metal, usually $Mn^{2+}$, e.g., $Cd_{1-x}Mn_xTe$. Among the fascinating properties which these Mn-based DMS alloys exhibit is giant Faraday rotation due to spin-spin exchange interaction between the $d$ electrons of $Mn^{2+}$ and the $s$-like ($p$-like) conduction-band (valence-band) electrons: the $sp$-$d$ exchange interaction. Large excitonic Faraday rotation was first observed by Gaj *et al.* in $Cd_{1-x}Mn_xTe$ (Ref. 1) and by Skowroński *et al.* in $Zn_{1-x}Mn_xTe$ (Ref. 2). More recently Bartholomew *et al.* have studied the Faraday effect in $Cd_{1-x}Mn_xTe$ and $Zn_{1-x}Mn_xTe$ over a wide range of Mn concentrations, temperature, and wavelengths,[3] while Butler has studied the Faraday rotation in $Cd_{1-x}Mn_xTe$ (Ref. 4). Kullendorff and Hök have investigated the temperature-independent Faraday rotation near the band gap in $Cd_{1-x}Mn_xTe$ (Ref. 5). Butler *et al.* have studied the frequency response of the Faraday rotation in $Cd_{1-x}Mn_xTe$ (Ref. 6). Faraday rotation has also been used to study the paramagnetic-to-spin-glass transition in $Hg_{1-x}Mn_xTe$ (Ref. 7) and $Cd_{1-x}Mn_xTe$ (Ref. 8). The Faraday effect in epitaxial films of $Cd_{1-x}Mn_xTe$ has been investigated by Koyanagi *et al.*[9] All of these materials have zinc-blende structure and, hence, the Faraday rotation that they exhibit is isotropic with respect to crystal orientation. The Faraday effect in a DMS having wurtzite hexagonal structure, e.g., $Cd_{1-x}Mn_xSe$, is expected to be anisotropic. We have investigated the Faraday effect in $Cd_{1-x}Mn_xSe$ for a wide range of $x$ and temperature. This paper presents the results of our investigation for magnetic fields along the optic axis. A proposed future publication will deal with results obtained with magnetic field perpendicular to the optic axis.

## II. EXPERIMENT

Single crystals of $Cd_{1-x}Mn_xSe$ were grown by the modified vertical Bridgman method. They were oriented by x-ray analysis using the Laue pattern technique to find the sixfold axis of symmetry, $\hat{\mathbf{c}}$. The manganese fraction $x$ was determined using electron-microprobe analysis. The sample surfaces were mechanically polished using successively finer grits down to 0.05-$\mu$m alumina powder. Before performing the measurements, the samples were prescreened to ensure that they were free from accidental birefringence even for $\mathbf{k}\|\hat{\mathbf{c}}$; such birefringence may have its origin in polycrystalline regions within the sample.

At room temperature, Faraday rotation was measured by placing the sample in a magnetic field of an electromagnet capable of attaining fields of up to 20 kG between two polaroid sheets set at 45° with respect to each other. The samples were oriented in the Faraday geometry, i.e., with $\mathbf{H}\|\mathbf{k}$, where $\mathbf{k}$ is the wave vector of the light. In this paper we report the results for the light sent along the optic axis, $\mathbf{k}\|\hat{\mathbf{c}}$; thus the natural birefringence characteristic of $Cd_{1-x}Mn_xSe$ does not play a role in the measurements. The incident photon energy was varied using a single-pass grating monochromator having a bandwidth of 10 meV, with a tungsten-halogen lamp serving as a light source. The transmitted light was detected with a silicon $p$-$i$-$n$ diode. The rotation was determined by

$$\sin(2\theta_F)=\frac{2I(H)-(I_a+I_b)}{I_a-I_b}\ , \tag{1}$$

where $\theta_F$ is the Faraday rotation angle, $I(H)$ is the transmitted intensity for a given magnetic field $H$, and $I_a$ ($I_b$) is the maximum (minimum) intensity as the analyzer

 

is rotated through 360°. This method can detect rotations as small as 0.1°. In general, $I_a$ and $I_b$ were measured at $H=0$ and were assumed not to vary with magnetic field. This is not true for photon energies near the band gap where $I_a$ can decrease ($I_b$ can increase) with $H$ due to circular dichroism, i.e., one circular polarization is preferentially absorbed. In these situations, the intensity exhibited many oscillations such that a Fourier transform of $I(H)$ versus $H$ could also be used to determine the fundamental frequency of oscillation, i.e., $\theta_F/H$. During the course of our investigations it was also found that, even for low photon energies, in many samples both $I_a$ and $I_b$ varied slightly with magnetic field. For some of these samples, the changes of $I_a$ and $I_b$ were periodic, with the same period as $I(H)$ versus $H$, and may be caused by residual birefringence due to internal strains, or because $\mathbf{k}$ may not be precisely parallel to $\hat{\mathbf{c}}$.[10] This effect causes the apparent rotation to deviate slightly from linear magnetic field dependence, most noticeably for $\theta_F$ around 45°, 135°, . . .; for example, the apparent rotation may be smaller (larger) than the true rotation as the true rotation approaches (exceeds) 45°. For rotations of less than 45° this effect could introduce small errors into our measurement of $\theta_F$, whereas for larger rotations this effect tends to "average out" when determining the slope of $\theta_F$ versus $H$.

For measurements at low temperatures, samples were placed in a variable-temperature optical cryostat equipped with a superconducting coil capable of attaining fields up to 60 kG, between two polarizing sheets oriented at 45°. White light from an incandescent lamp was passed through the sample and spectrally analyzed with a

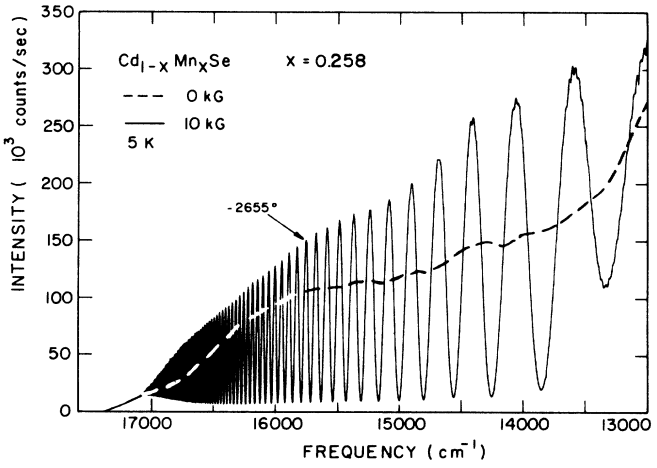


FIG. 1. Transmission with the polarizer and the analyzer axes at 45° with respect to each other in the Faraday configuration (Faraday intensity) as a function of frequency for $Cd_{1-x}Mn_xSe$, $x=0.258$, having a sample thickness of 3.026 mm, $T=5$ K, and $H=10$ kG (solid line). The transmission without magnetic field (dashed line) is also shown for comparison. Each successive maximum indicates an additional 180° of rotation; the maximum at 15 754 $cm^{-1}$ corresponds to a Faraday rotation of −2655°, while the magnitude of the rotation increases with increasing wave numbers.

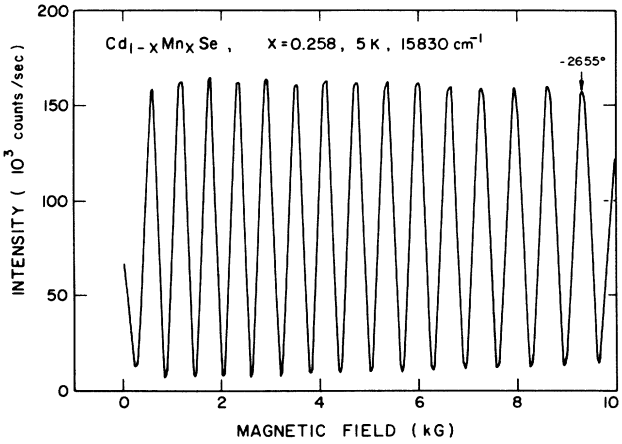


FIG. 2. Faraday intensity as a function of magnetic field for $Cd_{1-x}Mn_xSe$, $x=0.258$, at $T=5$ K and $E=15\,830$ $cm^{-1}$. The rotation is linear with magnetic field in the range examined; the magnetization will show saturation effects for $H>15$ kG. The value of the rotation at 10 kG is used to determine the absolute value of Faraday rotation in the transmission curve shown in Fig. 1.

double-monochromator operated with a typical resolution of 0.5 $cm^{-1}$ (0.06 meV). Care was taken that the sample was not heated by the incident light. In Fig. 1 we see the transmission for $Cd_{1-x}Mn_xSe$, $x=0.258$, at 5 K for $H=0$ and 10 kG. As can be seen, when the magnetic field is applied, the transmission spectrum shows oscillations; each successive maximum represents an additional Faraday rotation of 180°. The absolute values of the rotation angles were determined by fixing the spectrometer at a specific wave number and varying the magnetic field from 0 to **H**. In Fig. 2 we show a transmission curve obtained in this manner for the spectrum shown in Fig. 1. The decrease of the intensity near $H=0$ indicates that the sign of the rotation is negative.[11] Thus the value of the rotation for 10 kG at 15 754 $cm^{-1}$ is −2655°. The magnitude of the rotation increases with increasing wave number, and so the entire Faraday dispersion information can be obtained from Figs. 1 and 2.

## III. THEORY

The Faraday effect in an isotropic medium is the rotation of the plane of polarization of linearly polarized light propagating along the magnetic field in which the medium is placed. Faraday rotation $\theta_F$ is then given by the well-known expression

$$\theta_F=\frac{lE}{2\hbar c}(n_- - n_+)\ , \tag{2}$$

where $l$ is the distance in the medium traversed by the light, $E$ is the photon energy, $\hbar$ and $c$ have their normal meanings, and $n_\pm$ are the indices of refraction for the two circular polarizations whose electric fields are described by the unit vectors

$$\hat{\sigma}_\pm=\frac{1}{\sqrt{2}}(\hat{\mathbf{x}}\pm\hat{\mathbf{y}})e^{-i\omega t}\ .$$

The origin of the interband Faraday effect is the splitting of the interband transitions in a magnetic field. For photon energies close to the energy band gap the Faraday rotation is given by[3]

$$\theta_F = \frac{lE}{2\hbar c}\frac{\partial n}{\partial E}\Delta E_{ij} , \tag{3}$$

where $\partial n/\partial E$ describes the dispersion of the refractive index and $\Delta E_{ij}$ is the energy difference between band gap transitions observed in $\hat{\sigma}_+$ and $\hat{\sigma}_-$ polarizations. In a wurtzite structure Eqs. (2) and (3) have to be modified since, in an arbitrary direction of propagation, the state of polarization which can propagate without change of form is elliptical; however, for $\mathbf{H}\|\mathbf{k}\|\hat{\mathbf{c}}$, the case considered in this paper, Eqs. (2) and (3) and their significance remain the same. Figure 3 shows a schematic diagram of zone-center band extrema of $Cd_{1-x}Mn_xSe$ with and without a magnetic field parallel to $\hat{\mathbf{c}}$, and the circularly polarized interband transitions with $\mathbf{H}\|\hat{\mathbf{c}}$. In wurtzite DMS alloys the conduction-band minimum occurs at the zone center and has $\Gamma_7$ symmetry. The combination of crystal field and spin-orbit splitting leads to a zone-center $\Gamma_9$ valence-band maximum, below which lie two $\Gamma_7$ maxima. The exciton associated with the topmost $\Gamma_9$ valence-band maximum has been labeled the $A$ exciton in the literature, whereas that associated with the next-lower-lying $\Gamma_7$ maximum is labeled the $B$ exciton, and that lying lower still is the $C$ exciton. The valence-band maxima in Fig. 3 are therefore labeled $\Gamma_9(A)$, $\Gamma_7(B)$, and $\Gamma_7(C)$, respectively. In the Faraday geometry, transitions originating from the $\Gamma_9(A)$ and $\Gamma_7(B)$ valence bands and terminating at the conduction band give rise to four circularly polarized transitions, labeled here as $a$, $b$, $c$, and $d$. The effect of the $a$ and $d$ transitions on the Faraday rotation will be much larger than that of the $b$ and $c$ transitions due to the following factors: (a) $\Delta E_{ij}$ is larger for the $a$ and $d$ transitions, (b) the transition probabilities for $a$ and $d$ are presumably greater than those for $b$ and $c$, as in the case of $Cd_{1-x}Mn_xTe$ (Ref. 12); and (c) in $Cd_{1-x}Mn_xSe$, for photon energies less than the band gap, the $a$ and $d$ transitions have a greater influence on the dispersion of the index of refraction than do the $b$ and $c$ transitions because the $\Gamma_9$ valence-band maximum is closer to the conduction band than the other two valence-band maxima. For these reasons we will neglect the effect of the $b$ and $c$ transitions on the Faraday rotation.

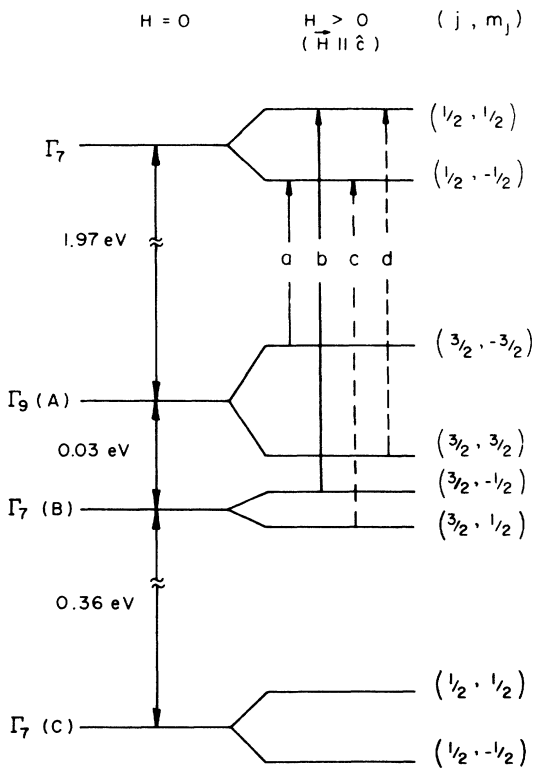


FIG. 3. Schematic diagram of conduction- and valence-band splittings and interband transitions for $Cd_{1-x}Mn_xSe$ in the Faraday configuration, with $\mathbf{H}\|\hat{\mathbf{c}}$; $\hat{\sigma}_+$ transitions ($a$ and $b$) are drawn with solid lines, whereas $\hat{\sigma}_-$ transitions ($c$ and $d$) are shown with dashed lines. The energy values are for $Cd_{1-x}Mn_xSe$, $x=0.10$ (Ref. 15).

The dispersion of Faraday rotation in $Cd_{1-x}Mn_xTe$ and $Zn_{1-x}Mn_xTe$ is much better explained in terms of an excitonic model than in terms of interband transitions.[1-3] For $Cd_{1-x}Mn_xSe$, excitonic transitions are also expected to dominate the Faraday rotation. For photon energies close to the energy band gap, we assume that the refractive index $n$ is given by $n^2=F_0(E_0^2-E^2)^{-1}$, where $F_0$ is a constant involving the oscillator strength of the excitonic transition and $E_0$ is the energy of the $A$ exciton. From Eq. (3) the Faraday rotation is given by

$$\theta_F = \left[\frac{\sqrt{F_0}\,l}{2\hbar c}\Delta E_0\right]\frac{1}{E_0}\frac{y^2}{(1-y^2)^{3/2}} , \tag{4a}$$

and the Faraday rotation per unit magnetic field per unit length, referred to as the Verdet constant $V$, is then

$$V = \frac{D}{E_0}\frac{y^2}{(1-y^2)^{3/2}} , \tag{4b}$$

where $y=E/E_0$ and

$$D = \frac{\sqrt{F_0}}{2\hbar c}\frac{\partial \Delta E_0}{\partial H} . \tag{4c}$$

For DMS alloys, the Zeeman splitting of the conduction and valence bands has two components: the intrinsic Zeeman effect, as seen in CdSe, and that due to the large $sp$-$d$ exchange interaction between the spins of the band electrons and those of the $Mn^{2+}$ ions. We shall consider the situation where the effect of the $sp$-$d$ exchange interaction dominates the Zeeman splitting of the $A$ exciton, i.e.,

$$\Delta E_0 = E_a(\hat{\sigma}_+) - E_d(\hat{\sigma}_-) = \frac{\beta-\alpha}{g_{Mn}\mu_B}M , \tag{5}$$

where $\alpha$ and $\beta$ are the $sp$-$d$ exchange integrals for the conduction- and valence-band electrons, respectively, $g_{Mn}=2$ is the Landé $g$ factor of the $Mn^{2+}$ spins, $\mu_B$ is the

Bohr magneton, and $M$ is the magnetization. Thus

$$\theta_F = \left[ \frac{\sqrt{F_0}\, l}{2\hbar c} \frac{\beta-\alpha}{g_{\mathrm{Mn}}\mu_B} M \right] \frac{1}{E_0} \frac{y^2}{(1-y^2)^{3/2}} . \quad (6)$$

The parameter $D$ is then

$$D = \frac{\sqrt{F_0}}{2\hbar c} \frac{\beta-\alpha}{g_{\mathrm{Mn}}\mu_B} \frac{\partial M}{\partial H} = \frac{\sqrt{F_0}}{2\hbar c} \frac{\beta-\alpha}{g_{\mathrm{Mn}}\mu_B} \chi , \quad (7)$$

where $\chi$ is the magnetic susceptibility per unit volume.

## IV. RESULTS AND DISCUSSION

Figure 1 shows Faraday rotation dispersion in $Cd_{1-x}Mn_xSe$, $x=0.258$, at 5 K for $H=10$ kG (solid line). Near the absorption edge, Faraday rotation is about 10 000°, which is several orders of magnitude larger than the rotation seen in CdSe, even close to the absorption edge. The rise of the envelope of the transmission minima near the absorption edge is due to circular dichroism and accidental strain birefringence, whereas that at low frequencies is due to the degradation of the polaroid response. Faraday rotation as a function of magnetic field for the same sample at 15 830 $cm^{-1}$ is seen in Fig. 2. The Faraday rotation increases linearly with magnetic field up to 10 kG; for higher fields there is some saturation of the rotation. As seen in this figure, the intensity at the first minimum near $H=0$ is higher than the other minima. This unexplained phenomenon was not seen at room temperature, but appeared in every sample in varying degree at lower temperatures; for some samples (especially for $x>0.25$) this phenomenon increased with decreasing temperature.

### A. The role of magnetization

According to Eq. (6), the Faraday rotation is proportional to the magnetization; in this section we investigate this relationship.

In Fig. 4 we see the Verdet constant as a function of photon energy at 295 K for $Cd_{1-x}Mn_xSe$, $x=0$ to 0.10. With no manganese present, the Verdet constant is positive over the entire spectral region investigated; this is similar to the behavior of other II-VI compounds.[13,14] For $x=0.01$, the Verdet constant is positive for low photon energies, but becomes negative near the energy band gap. For values of $x>0.05$ the value of the Verdet constant is negative for the entire spectral region, and its dispersion is increasingly excitonic in nature. The change of the sign of the Verdet constant demonstrates the competition between the positive interband Faraday rotation (possibly derived from transitions at $k\neq 0$ as well as transitions between energy bands in the crystal other than the valence and conduction bands) and the negative rotation derived from excitonic transitions at the zone center, $k=0$. The sign of the excitonic rotation is given by the sign of $\beta-\alpha$ [see Eq. (6)], which is $-1.37$ eV for $Cd_{1-x}Mn_xSe$ (Ref. 15) and, hence, the excitonic rotation is expected to be negative.

The magnetization for a very dilute system of $Mn^{2+}$ spins is, to a good approximation, given by

$$M = -g_{\mathrm{Mn}}\mu_B x N_0 \langle S_z \rangle_{\mathrm{Mn}} \text{ and } \langle S_z \rangle_{\mathrm{Mn}} = -\tfrac{5}{2} B_{5/2}(\eta) , \quad (8)$$

where $\langle S_z \rangle_{\mathrm{Mn}}$ is the thermal average of the $Mn^{2+}$ spins along the direction of the applied magnetic field, $\eta = g_{\mathrm{Mn}}\mu_B H/k_B T$, $k_B$ is the Boltzmann constant, and $B_{5/2}$ is the Brillouin function $B_J$ for $J=\frac{5}{2}$ (Ref. 16). The effect of the weak antiferromagnetic coupling between the $Mn^{2+}$ can be empirically taken into account by introducing two phenomenological constants: replacing $x$ by an effective manganese fraction $\bar{x}$ and replacing $T$ by an effective temperature $T+T_{\mathrm{AF}}$ (Ref. 17). The Brillouin function will saturate for large values of $\eta$. Hence, the magnetization saturates for high magnetic field and/or low temperature. This behavior is strikingly manifested in the Faraday rotation of $Cd_{1-x}Mn_xSe$. Figure 5 shows

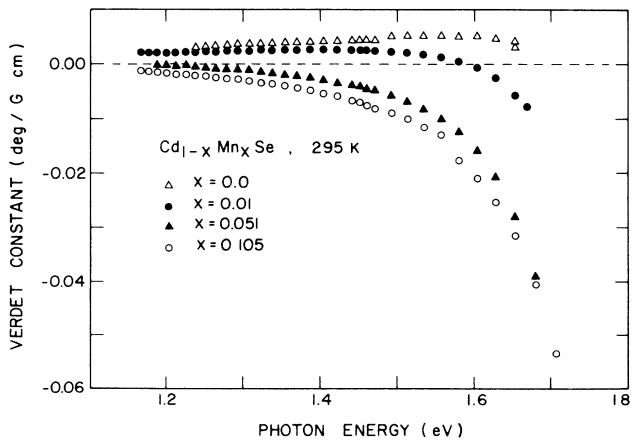


FIG. 4. Verdet constant dispersion in $Cd_{1-x}Mn_xSe$ at room temperature for several low values of $x$, showing the sign reversal of the Faraday rotation.

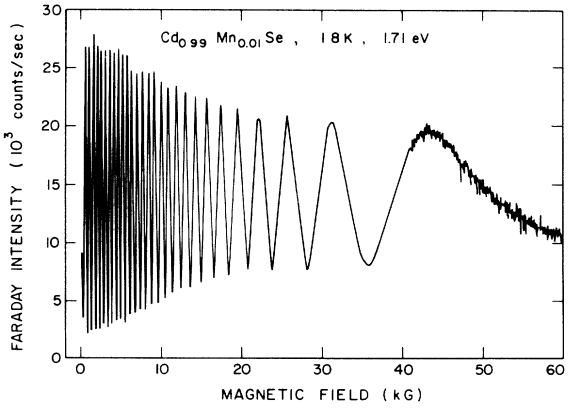


FIG. 5. Faraday intensity as a function of magnetic field for $Cd_{1-x}Mn_xSe$, $x=0.01$, having a thickness of 2.925 mm at $T=1.8$ K and $E=1.71$ eV, demonstrating the effect of the saturation of the magnetization on the Faraday rotation. The effect of Faraday ellipticity (circular dichroism) can also be seen in the data.

the "Faraday" intensity, i.e., the transmitted intensity in the Faraday geometry, obtained in the same manner as Fig. 2, for $Cd_{1-x}Mn_xSe$, $x=0.01$, at 1.8 K and $E=1.71$ eV. For low magnetic field, the period of the oscillations is constant, whereas for high magnetic fields this period increases dramatically as the magnetization saturates. We found that the rotation as a function of magnetic field can be fitted to the form $\theta_F=-5232°B_{5/2}(\eta)$, assuming $T=2.3$ K; notice that this temperature is higher than 1.8 K, implying that $T_{AF}=0.5$ K, thus showing that even for very dilute DMS alloys the exchange coupling between the $Mn^{2+}$ ions is manifested. In addition, the amplitude of the oscillations decreases, demonstrating the effect of "Faraday ellipticity," i.e., the transmitted light exits the medium elliptically polarized due to circular dichroism.

The dramatic temperature dependence of the magnetization, as seen through the Faraday rotation, is displayed in Fig. 6. Here the Faraday intensity is shown as a function of inverse temperature for $Cd_{1-x}Mn_xSe$, $x=0.258$, at a magnetic field of 10 kG (the Faraday intensity was recorded as the sample was slowly cooled in a magnetic field); we note that for $H<12$ kG the magnetization is linear with magnetic field for $T>5$ K, i.e., $\eta\ll 1$. The intensity oscillates with the period gradually increasing with increasing $T^{-1}$. According to Eq. (6), the temperature dependence of both the magnetization and $E_0$ (hence $y$) will affect the Faraday rotation. The effect of the change in $E_0$ as a function of temperature is minimized by collecting data at a constant $E/E_0$; the value of $E_0^{-1}$ changed by less than 3% from 200 to 5 K. Thus the temperature dependence of $\theta_F$ reflects the temperature dependence of $M$. The increasing period of oscillation in Fig. 6 indicates that the magnetization varies slower than $T^{-1}$, i.e., it is inversely proportional to an "effective temperature," as discussed earlier.

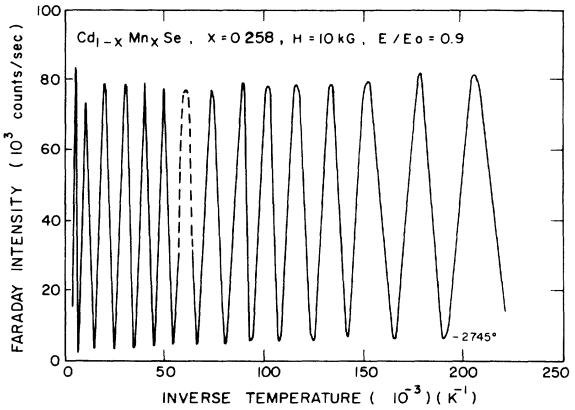


FIG. 6. Faraday intensity as a function of inverse temperature for $Cd_{1-x}Mn_xSe$, $x=0.258$, at $H=10$ kG. Photon energy $E$ was constantly changed so that the ratio $E/E_0$ remains 0.9. In this way, the increasing rotation very closely reflects the increase of the magnetization with decreasing temperature. The dashed section of the curve around $60\times10^{-3}$ $K^{-1}$ is a reconstruction of the oscillation maximum which could not be recorded during the measurement.

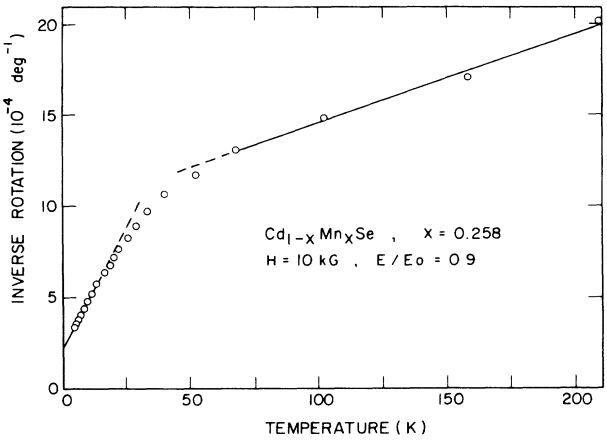


FIG. 7. Inverse Faraday rotation as a function of temperature for $Cd_{1-x}Mn_xSe$, $x=0.258$, at $H=10$ kG, derived from the data shown in Fig. 6. This reflects the temperature dependence of inverse magnetization. The extrapolation of the data for $T>70$ K gives a Curie-Weiss temperature ($T_{CW}$) of 196±12 K. The extrapolation of the data for 5 K $\leq T\leq 20$ K indicates the value of $T_{AF}$ is 7.1 K in this temperature region.

In Fig. 7 we plot the inverse $\theta_F$ as a function of temperature, representing the data shown in Fig. 6. For high temperatures, the plot follows a Curie-Weiss behavior. An extrapolation of the data indicates a Curie-Weiss temperature ($T_{CW}$) of 196±12 K, in excellent agreement with that determined by magnetic susceptibility measurements.[18] As the temperature decreases, the plot shows a down-turn toward the origin, also characteristic of the magnetic susceptibility of DMS alloys. Notice that for temperatures between 5 and 20 K the inverse rotation is empirically found to be proportional to $T+T_{AF}$ and indicates that $T_{AF}$ is 7.1±0.1 K. This value of $T_{AF}$ agrees well with the value of $T_{AF}$ found by fitting the Faraday

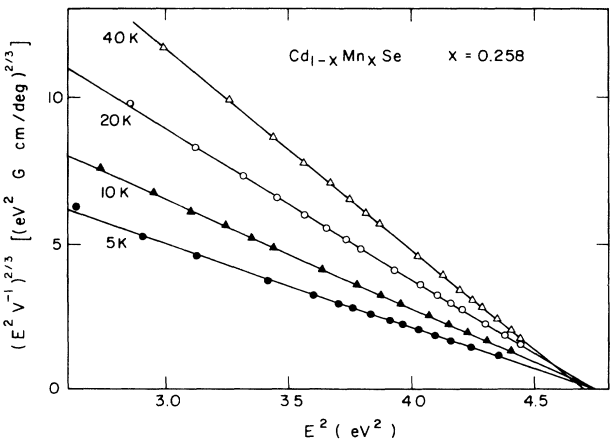


FIG. 8. $(E^2V^{-1})^{2/3}$ vs $E^2$ for $Cd_{1-x}Mn_xSe$, $x=0.258$, for several temperatures, demonstrating the excellent fit of the Faraday rotation dispersion to the excitonic (single oscillator) model [see Eq. (4b)].

rotation dispersion to a single oscillator model, as discussed below. In order to follow the evolution of $T_{AF}$ at low temperatures into the Curie-Weiss temperature regime, one has to take into account the temperature dependence of $\bar{x}$. In the absence of quantitative knowledge of this temperature dependence, we view $T_{AF}$ as merely an empirical coefficient, which is a function of $x$ *and* $T$, giving the profile of $M$ versus $H$ for a given $x$ and $T$ (Refs. 3 and 18).

### B. The excitonic model

As explained in Sec. III, excitonic transitions play a dominant role in Faraday rotation of DMS alloys. The dispersion of the Verdet constant, according to the excitonic model, is given by Eq. (4b). Thus plotting $(E^2V^{-1})^{2/3}$ *versus* $E^2$ will yield a straight line whose intercept with the $E^2$ axis determines $E_0$, while the slope gives $D$. Such plots, including linear fits, are shown in Fig. 8 for $Cd_{1-x}Mn_xSe$, $x=0.258$, at various temperatures. The raw data for the 5-K plot in this figure are displayed in Fig. 1. As can be seen, the excitonic model fits the observed Verdet constant dispersions extremely well over the entire spectral range. The linear fits of room temperature data and for $Cd_{1-x}Mn_xSe$ with $x \leq 0.01$, even at low temperatures, are not normally as good as those at low temperature with $x > 0.01$. This indicates that the excitonic model is most successful when the diamagnetic contribution to the rotation is negligible compared with the paramagnetic contribution due to $Mn^{2+}$ ions.

Figure 9(a) shows a plot of $E_0$, determined from fitting Faraday rotation to the excitonic model, as a function of temperature for a wide range of $x$. For $T \geq 40$ K, $E_0$ decreases linearly with increasing temperature. The $x$ dependence of $\partial E_0/\partial T$ was found to be $-(2.8+10.6x)\times 10^{-4}$ eV/K, ,which is in reasonable agreement with that found by piezomodulated reflectivity studies.[19,20] For $T < 40$ K, many of the curves show the nonlinear temperature dependence of $E_0$.

TABLE I. Temperature and Mn concentration dependence of $E_0$ in $Cd_{1-x}Mn_xSe$. $A$-exciton energy determined by piezomodulated reflectivity (Ref. 19).

| $T$ (K) | $E_0$ (eV) | $E_A$ (eV) |
|---|---|---|
| 300 | $1.732+1.11x$ | $1.743+1.16x$ |
| 80 | $1.795+1.33x$ | $1.807+1.34x$ |
| 10 | $1.813+1.41x$ | $1.817+1.42x$ |
| 5 | $1.814+1.40x$ | |

Figure 9(b) shows the $x$ dependence of $E_0$ for 5, 80, and 295 K. Included in this figure are linear fits of these data. The fitting parameters are displayed in Table I. Also shown in this table are $x$ dependences of the $A$ exciton as determined by piezomodulated reflectivity. Once again the agreement is quite good.

Figure 10 shows the inverse of $D$ as a function of temperature for a variety of manganese concentrations. For the high temperature region, corresponding to Fig. 10(a), $D^{-1}$ increases with increasing temperature. The slope of these curves decreases with increasing $x$ up to $x=0.25$, beyond which the slope varies little. For the low temperature region, Fig. 10(b), a similar behavior is seen, although for $x > 0.4$, $D^{-1}$ does not increase linearly with temperature.

Using Eq. (7) and the Curie-Weiss law,[18] $D$ in the high temperature region is given by

$$D=\frac{35}{12}\frac{\sqrt{F_0}}{2\hbar c}\frac{g_{Mn}\mu_B N_0(\beta-\alpha)x}{k_B(T+T_{CW})} \tag{9}$$

and, so $D^{-1}=m_1(T+T_{CW})$, where $m_1$ is inversely proportional to $x$. A plot of $D(T+T_{CW})$ is reasonably linear with $x$ (the values of $T_{CW}$ being given in Ref. 18).

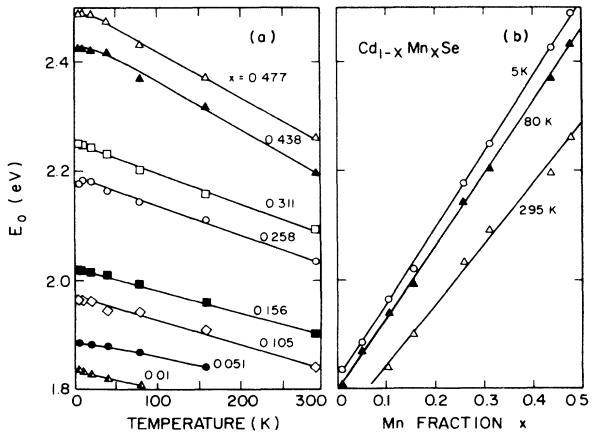


FIG. 9. Temperature and manganese fraction ($x$) dependence of $E_0$. $E_0$ was obtained from linear fits of Verdet constants using the excitonic model; see, for example, Fig. 8. Table I lists the variation of $E_0$ with $x$.

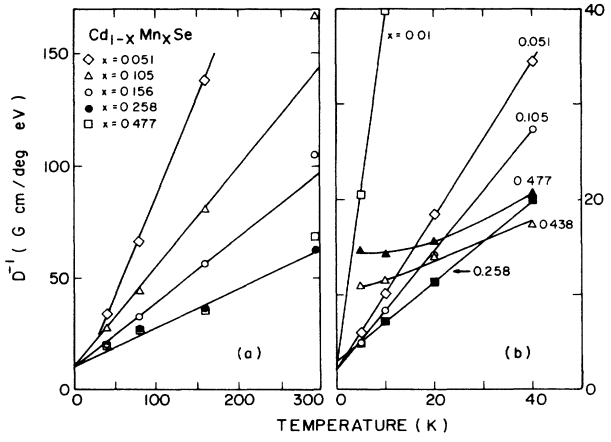


FIG. 10. $D^{-1}$ as a function of temperature for $T \geq 40$ K (a) and for $T \leq 40$ K (b) in $Cd_{1-x}Mn_xSe$, for several values of $x$. The slope of each figure corresponds to $m_1$ and $m_2$, respectively. The values of $m_2$ are listed in Table II.

Therefore the small change of $D^{-1}$ with $x$ for $x > 0.25$ is due to the increase of the $T_{CW}$ with increasing $x$. Strictly speaking, the Curie-Weiss law holds only at a temperature higher than $T_{CW}$, although in practice the magnetic susceptibility follows the Curie-Weiss law even down to temperatures below $T_{CW}$ (Ref. 18). This is evident in Fig. 7, but at temperatures lower than 70 K, $\theta_F^{-1}$ (and hence $\chi^{-1}$) starts deviating from the Curie-Weiss behavior.

Note that the value of $D^{-1}$ at 300 K is always higher than that extrapolated from data at lower temperatures. This is probably due to the diamagnetic contribution to the Faraday effect which is not included in Eq. (9). The diamagnetic contribution is more significant for higher temperatures and/or for lower manganese concentrations, where the effect of *sp-d* exchange interaction is small.

$D$ in a low temperature region, using Eqs. (7) and (8), is given by[3]

$$D = \frac{35}{12}\frac{\sqrt{F_0}}{2\hbar c}\frac{g_{Mn}\mu_B N_0(\beta-\alpha)\bar{x}}{k_B(T+T_{AF})} \tag{10}$$

and, so, $D^{-1}$ has the form of $m_2(T+T_{AF})$. The slope $m_2$ is different from $m_1$, as expected by the departure of $\chi$ from Curie-Weiss behavior at low temperature (see Fig. 7). Due to the phenomenological nature of $\bar{x}$ and $T_{AF}$, these parameters exhibit certain implicit dependence on several factors. For example, the ratio $\bar{x}/x$ decreases with increasing $x$, indicating increased antiferromagnetic coupling between neighboring $Mn^{2+}$ ions (in the form of spin complexes—pairs, triplets, etc.).[21] This explains why $m_2$ is not quite inversely proportional to $x$. The values of $T_{AF}$ obtained from our data, neglecting the temperature dependence of the $\bar{x}$, are given in Table II. The increase of the $T_{AF}$ with increasing $x$ is also qualitatively due to an increasing number and variety of antiferromagnetic spin complexes.[22]

DMS alloys can exhibit a paramagnetic to spin-glass transition characterized by a cusp in $\chi$ at low temperatures. The temperature $T_c$ at which this cusp occurs increases with $x$. As we have previously mentioned, $D$ is proportional to $\chi$ and, so, curves of $D$ (or $D^{-1}$) versus $T$ should also display a cusp at $T = T_c$. Indeed, Faraday rotation has been used to study the magnetic phase transition.[7,8] The curves in Fig. 10(b) do not clearly show this behavior since, as the data were taken, the magnetic field was varied at each temperature; this was done in order to determine the absolute values of the Faraday rotations. It is well known that magnetic susceptibility curves in spin-glass state depend on the thermal and magnetic history of the sample. For example, a curve of $\chi$ versus $T$ for a sample cooled in zero field will be different from that cooled with a field present. Kierzek-Pecold *et al.*[8] observed a dramatic decrease in $\theta_F$ in $Cd_{1-x}Mn_xTe$ for $T < T_c$ upon zero-field cooling, whereas $\theta_F$ was nearly independent of $T$ for $T < T_c$, upon field cooling. They also claimed that for $T < T_c$ the field-cooled-like situation can be obtained from a zero-field cooled sample by applying a field for a very long time (in their case, the time was 150 min). Since our Faraday rotation measurements commonly took in excess of 30 min to complete, it is not unexpected that the curves in Fig. 10(b) for $x > 0.4$ more closely resemble their field-cooled measurements and do not show a distinct cusp.

Both hysteresis and time dependence of the magnetization are expected in a spin-glass phase.[23] Figure 11 shows the low-field portion of the hysteresis of the Faraday rotation in $Cd_{1-x}Mn_xSe$, $x = 0.48$, for $T = 5$ K in the spin-glass state. The sample was cooled in zero magnetic field from room temperature to 5 K, after which the external magnetic field was increased to 60 kG. Then the magnetic field was reduced to 0 kG (solid circles), and the magnetic field was reversed, starting from 0 to $-60$ kG (open circles). The field was brought from $-60$ to 0 kG (open

TABLE II. Linear least-squares-fit parameters for $D^{-1}$ vs $T$ ($T \leq 40$ K), see Eq. (10).

| $x$ | $m_2$ (G cm/deg eV K) | $T_{AF}$ (K) |
|---|---|---|
| 0.01 | −4.45 | 0.5 |
| 0.051 | −0.81 | 2.6 |
| 0.105 | −0.64 | 2.8 |
| 0.156 | −0.53 | 4.1 |
| 0.258 | −0.43 | 6.5 |
| 0.311 | −0.36 | 12.9 |

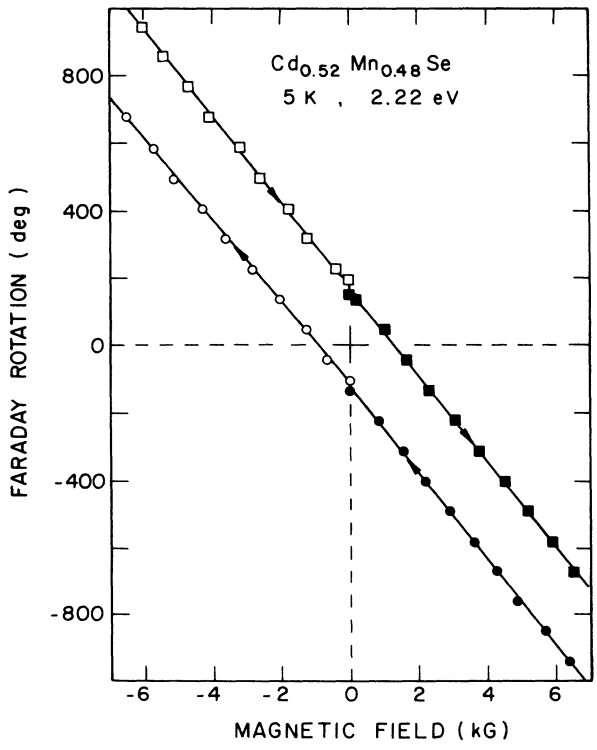


FIG. 11. Faraday rotation as a function of magnetic field for $Cd_{1-x}Mn_xSe$, $x = 0.48$, with a thickness of 4.971 mm at $T = 5$ K and $E = 2.22$ eV, demonstrating the hysteresis of the Faraday rotation in spin-glass state. The magnetic field was swept between 0 and ±60 kG, although only the low field data are displayed to show the hysteresis more clearly.

squares), and again was reversed and increased to 60 kG (solid squares). Hysteresis effects are clearly evident in that $\theta_F(H=0)$ for the sweep down differs from $\theta_F(H=0)$ for the return sweep by some 300°. Note the small discontinuity in the rotation angle as it passes through 0 kG. This effect is a result of a relaxation of the magnetization (hence $\theta_F$) during the few minutes in which the superconducting magnetic leads were reversed.

## V. CONCLUDING REMARKS

We have studied the Faraday rotation in $Cd_{1-x}Mn_xSe$ for $\mathbf{k}\|\hat{\mathbf{c}}$ over a wide range of manganese concentration and temperature. The behavior of the Faraday effect in this configuration is identical with that of an isotropic material. At room temperature, the Faraday rotation in CdSe is positive for all the photon energies investigated. For very small $x$ ($x<0.05$), the rotation is positive for low photon energies, but becomes negative as the photon energy approaches that of the band gap. As $x$ increases, the rotation becomes less positive and is eventually negative for all frequencies; the paramagnetic rotation of the $Mn^{2+}$ ions eventually dominates the intrinsic diamagnetic rotation of CdSe. As the temperature decreases the magnitude of the rotation increases dramatically, yielding thousands of degrees of rotation for modest magnetic fields and sample thicknesses; this giant Faraday rotation is due to the *sp-d* exchange interaction. For high magnetic fields the rotation exhibits saturation effects as a result of the Brillouin-function-like behavior of the magnetization. The dispersion of the rotation is well described by a single oscillator (excitonic) model. This analysis yields the excitonic energy as a function of temperature and Mn concentration. We also obtain information about the magnetic susceptibility, including the antiferromagnetic temperature ($T_{AF}$), and evidence of magnetic freezing for large $x$ and low temperature. When the sample is in the spin-glass magnetic phase, the Faraday rotation exhibits hysteresis upon reversing the magnetic field. Experiments are in progress for the magnetic field perpendicular to the $c$ axis, where the natural birefringence of $Cd_{1-x}Mn_xSe$ must be taken into account. This will be reported later.

## ACKNOWLEDGMENTS

The work reported in this paper was supported by National Science Foundation Grant No. DMR-85-20866 and the Defense Advanced Research Foundation Agency (DARFA)–University Research Initiative (URI) Consortium "Diluted Magnetic Semiconductors and their Heterostructures" administered by the U.S. Office of Naval Research (Contract No. N00014-86-K-0760).

[1]J. A. Gaj, R. R. Gałazka, M. Nawrocki, and J. Ginter, in Materialy VIII Ogólnokrajowego Seminarium Zwiazków Półprzew., Jaszowiec, 1977 [Pr. Inst. Fiz. Polska Akad. Nauk Warszawa **75**, 112 (1978)]; J. A. Gaj, R. R. Gałazka, and M. Nawrocki, Solid State Commun. **25**, 193 (1978).

[2]M. Skowroński, J. M. Baranowski, and L. J. Ludwicki, in Materialy VIII Ogólnokrajowego Seminarium Zwiazków Półprzew., Jaszowiec, 1977 [Pr. Inst. Fiz. Polska Akad. Nauk Warszawa **75**, 127 (1978)].

[3]D. U. Bartholomew, J. K. Furdyna, and A. K. Ramdas, Phys. Rev. B **34**, 6943 (1986).

[4]M A. Butler, Solid State Commun. **62**, 45 (1987).

[5]N. Kullendorff and B. Hök, Appl. Phys. Lett. **46**, 1016 (1985).

[6]M. A. Butler, S. J. Martin, and R. J. Baughman, Appl. Phys. Lett. **49**, 1053 (1986).

[7]A. Mycielski, C. Rigaux, M. Menant, T. Dietl, and M. Otto, Solid State Commun. **50**, 257 (1984).

[8]E. Kierzek-Pecold, W. Szymanska, and R. R. Gałazka, Solid State Commun. **50**, 685 (1984).

[9]T. Koyanagi, K. Matsubara, H. Takaoka, and T. Takagi, J. Appl. Phys. **61**, 3020 (1987).

[10]Faraday rotation in a birefringent medium can be analyzed using the Poincaré sphere; see, for example, G. N. Ramachandran, and S. Ramaseshan, J. Opt. Soc. Am. **42**, 49 (1952).

[11]The sign of the rotation is positive for counterclockwise rotations when viewing against $\mathbf{k}$ and $\mathbf{H}\|\mathbf{k}$.

[12]J. A. Gaj, J. Ginter, and R. R. Gałazka, Phys. Status Solidi B **89**, 655 (1978).

[13]A. Ebina, T. Koda, and S. Shionoya, J. Phys. Chem. Solids **26**, 1497 (1965).

[14]M. Balkanski, E. Amzallag, and D. Langer, J. Phys. Chem. Solids **27**, 299 (1966).

[15]R. L. Aggarwal, S. N. Jasperson, J. Stankiewicz, Y. Shapira, S. Foner, B. Khazai, and A. Wold, Phys. Rev. B **28**, 6907 (1983).

[16]We follow the notation for $\eta$ used in F. Reif, *Fundamentals of Statistical and Thermal Physics* (McGraw-Hill, New York, 1965), p. 259.

[17]J. A. Gaj, R. Planel, and G. Fishman, Solid State Commun. **29**, 435 (1979); AF denotes antiferromagnetic.

[18]J. Spałek, A. Lewicki, A. Tarnawski, J. K. Furdyna, R. R. Gałazka, and Z. Obuszko, Phys. Rev. B **33**, 3407 (1986).

[19]Y. R. Lee, A. K. Ramdas, and R. L. Aggarwal, Phys. Rev. B **38**, 10 600 (1988).

[20]W. M. Becker, in *Diluted Magnetic Semiconductors*, Vol. 25 of *Semiconductors and Semimetals*, edited by R. K. Willardson and A. C. Beer (Academic, New, York, 1988), p. 51.

[21]Y. Shapira, S. Foner, D. H. Ridgley, K. Dwight, and A. Wold, Phys. Rev. B **30**, 4021 (1984).

[22]G. Barilero, C. Rigaux, N. H. Hau, J. C. Picoche, and W. Giriat, Solid State Commun. **62**, 345 (1987).

[23]D. Chowdhury and A. Mookerjee, Phys. Rep. **114**, 1 (1984). See Sec. 2.2 on "Magnetization and susceptibility measurements."